Materials Express

Article

Production and enzymatic degradation of poly(ε-caprolactone)/graphene oxide composites

V. Martínez-Ramón[1], I. Castilla-Cortázar[1], A. Vidaurre[1,2], and A. J. Campillo-Fernández[1,*]

[1]Centre for Biomaterials and Tissue Engineering, CBIT, Universitat Politècnica de València, 46022 Valencia, Spain
[2]CIBER de Bioingeniería, Biomateriales y Nanomedicina (CIBER-BBN), Madrid, 28029, Spain

ABSTRACT

Poly(ε-caprolactone) (PCL) based composites containing different graphene oxide (GO) contents (0.1, 0.2 and 0.5 wt%) were produced by the solution mixing method followed by compression molding and enzymatically degraded in a pH 7.4 phosphate buffer solution containing *Pseudomonas lipase* at 37 °C. Morphological changes, molecular weight, calorimetric and mechanical properties were analyzed according to graphene oxide content. The study of tensile properties showed that the composites increased their Young's modulus, while tensile strength and elongation at break decreased to significantly less than that of neat PCL. PCL composite crystallinity was evaluated by differential scanning calorimetry (DSC). It was found that incorporating GO can reduce nucleation activity as well as crystallization rates, from 67.6% for neat PCL to 50.6% for a composite with 0.5 wt% GO content. For enzymatic degradation, the weight loss data showed that incorporating GO into the PCL significantly altered enzymatic degradation. The presence of GO did not alter PCL's hydrolysis mechanism, but did slow down composite enzymatic degradation in proportion to the percentage of filler content.

Keywords: Polycaprolactone, Graphene Oxide, Enzymatic Degradation, *Pseudomonas lipase*, Molecular Weight, Morphology, Mechanical Properties.

1. INTRODUCTION

PCL and other biodegradable polyesters are being produced on a semi-commercial scale in order to solve at least part of the problem of plastic waste accumulation. The polyesters also have the additional advantage that almost all the monomers used in their preparation can be obtained from renewable resources [1–2]. PCL is a hydrophobic, semi-crystalline polymer with a crystallinity that tends to fall as molecular weight is raised. It has good solubility, a low melting point (59–64 °C) and its excellent blend-compatibility has made it the subject of many studies on potential biomedical applications, including drug delivery and bone repair, as it is compatible with both hard and soft materials [3–4].

Choosing the right biomaterial is essential to the success of tissue engineering applications [5–6]. The design and development of multi-component polymer systems is a suitable method of developing innovative multifunctional biomaterials, as conventional polymer materials with only one component cannot be used in all cases [7–10]. Introducing nanofillers into biodegradable polymer is a particularly promising method of obtaining nanocomposites with specific tissue engineering properties [11]. Polymer nanocomposites can be obtained by combining polymer and inorganic/organic fillers on the nanometer scale [12–13]. These nanofillers are classified into different categories according to their dimensions: nanoparticles, nanotubes, and nanolayers [2]. Graphene-derived fillers are also promising polymer fillers due to their functional groups on the surface of graphene sheets, which can facilitate their compatibility with the polymer matrix.

GO, a widely studied form of graphene, contains a single layer of carbon atoms obtained from an original

---

*Author to whom correspondence should be addressed.

Production and enzymatic degradation of poly(ε-caprolactone)/GO composites
Martínez-Ramón et al.

Materials Express

graphene lattice that has been oxidized to form C–O bonds [14]. In its bulk form, known as *graphite oxide*, it has been a popular subject of study since Brodie first synthesized it in 1885 [15]. Several models of the GO structure have been developed, which often partially exclude each other, but despite the effort, its structure has remained elusive [16] and a matter of debate [17]. It is thought that hydroxyl and epoxy groups are present in the highest concentration on the basal plane, with carboxylic acid groups around the sheet periphery. GO has an expanded interlayer spacing relative to graphite, which depends on humidity due to intercalation of water molecules [18] and makes it highly hydrophilic [14, 19]. The functional groups found on the surface of GO sheets, such as carboxyl, hydroxyl and epoxide, improve its dispersibility in organic solvents [20]. It also has good processability since it interacts well with organic polymers [18, 21].

The essential requirement for obtaining hybrid materials is that the reinforcement disperses correctly in the matrix, as well as ensuring that the components interact well [18, 20–29]. In recent years, a variety of processing methods have been proposed to disperse graphenes in polymer matrices, e.g., *in situ* polymerization, melt blending and solution mixing [30–33]. Solution mixing involves an additive dispersing phase, then dissolving the matrix polymer in co-solvents to recover the composites by evaporating the solvent or coagulating it with non-solvents. This approach can disperse the particles better than melt processing, although the particles may reaggregate due to slow solvent evaporation. Its main advantage is that it can synthesize polymer-based intercalated nanocomposites with low or even no polarity [21]. The different processes have been shown to cause different degrees of nanofiller dispersion in the matrix and thus have different effects on the properties of polymer composites [34–35]. Sonication or high-speed shearing in conjunction with solution-phase mixing has been proposed to enhance dispersity and give GO better solubility with non-polar solvents [36].

GO has also been used as a filler material for polymers, since it was found to improve its mechanical and electrical properties at low filler loadings [37]. Wan and Chen produced PCL/GO films with various 0.3–2 wt% GO loadings by solvent casting before compression molding to study their mechanical properties and bioactivity; the resulting PCL/GO composites showed that GO's reinforcing effect on PCL could be attributed to the strong interfacial interactions between both phases, characterized by Fourier transform infrared spectroscopy [38]. PCL and GO composites were successfully synthesized by ring opening polymerization of ε-caprolactone with GO as the initiator. GO was found to have an astounding effect on PCL crystallization due to its good dispersion in the composite [39]. Kumar et al. showed how reduced GO and amine-functionalized GO affected the dynamic mechanical behavior, wettability and stem cell response of compression-molded PCL

composites [40], while Song et al. produced a series of electrospun PCL/GO scaffolds; the addition of low-concentration GO improved the mechanical properties and the overall morphologies of PCL/GO composite nanofiber scaffolds [41]. Ramazani and Karimi incorporated GO and reduced GO nanofillers into PCL, followed by electrospinning and created electrically conducting scaffolds [42].

Although much work has been done on preparing graphene derivative composites, less attention has been given to the biodegradation of these materials [43–44]. The polyester degradation mechanism takes place in two steps, random hydrolysis ester cleavage and weight loss through the diffusion of oligomeric sort from the volume [45]. It is accepted that in the later stages of *in vivo* degradation, enzymatic activity is involved [46]. Polyesters' enzymatic degradation depends on their chemical structure, the hydrophilic/hydrophobic balance of the main chain, molecular weight, specific solid-state morphology and crystallinity, among others. The degradation rate can also be affected by certain aspects of the crystalline structure and morphology, such as spherulite size and lamellar structure [47]. The enzymatic degradation of PCL polymers has been mostly studied, especially in the presence of lipase-type enzymes [48–52]. Three types of lipase have been reported to significantly accelerate PCL degradation: *Rhizopus delemer lipase* [53–54], *Rhizopus arrhizuslipase* [50], and *Pseudomonas lipase* [47, 48, 51]. Pristine, highly crystalline PCL, was reported to totally degrade in 4 days in the presence of *Pseudomonas* (PS) *lipase* [48–49], in contrast to hydrolytic degradation in the absence of enzymes, which lasts more than two years [49, 55].

In a previous in-depth study, a number of nanocomposites produced by the solution mixing method with various graphene oxide filler contents were analyzed for possible use in biomedical applications; the aspects studied included morphological changes, crystallization, infrared absorbance, molecular weight, thermal properties, and biocompatibility, according to the GO content [56]. The method of sample preparation we report here includes some refinements with respect to the previous work in relation to improving GO dispersion through sonication and press molding [56]. Some previous studies analyzed the influence of enzymatic degradation on different samples based on pure PCL [57] and the accelerated degradation at extreme pHs of pure PCL without GO [58]. In this work we studied the enzymatic degradation of a series of PCL/GO hybrids containing different graphene oxide filler concentrations (0, 0.1, 0.2 and 0.5 wt% of GO) to gain a better understanding of the degradation process. An in-depth study was made of morphology, weight loss, molecular weight distribution analyzed by gel permeation chromatography (GPC), thermal and mechanical properties as a function of GO content.

Article

Materials Express

Production and enzymatic degradation of poly(ε-caprolactone)/GO composites
Martínez-Ramón et al.

Article

2. EXPERIMENTAL DETAILS

2.1. Materials

PCL pellets (Polysciences) ($M_w = 43.000$–50.000), diox-ane solvent (Fisher) and powdered graphene oxide (Graphenea) were all used as received. According to company information, GO was obtained from graphite which was chemically processed to obtain monolayer flakes. Lipase from *Pseudomonas* (powder, EC3.1.1.3., 40 units/mg) was purchased from Sigma Aldrich, sodium azide (NaN$_3$) 99% from Aldrich, phosphate buffer saline, PBS 1× solution, pH 7.4, from Fisher and type I ultrapure water from a Direct-Q 3 water purification system (Merck Millipore).

2.2. PCL/GO Composites Preparation

A mixture of powdered GO and type I ultrapure water were sonicated for 2 hours in a Sonopuls ultra-sonic homogenizer (Bandelin HD3200) operating at a high-frequency power of 100 W, pulsation time on/off 0.5/0.5 seconds, respectively, equipped with a TT13FZ probe. In order to dissipate the internal heat induced by sonication, the mixture was placed in a glass containing ice that was replaced at 10-minute intervals. The mixture was centrifuged in an Eppendorf 5804R at 10000 rpm for 10 minutes. The supernatant was retired and the precipitate was placed in a petri dish under vacuum at 40 °C. PCL/GO samples were prepared by solution mixing followed by solvent evaporation as follows: PCL pellets were dis-solved in dioxane, after which three solutions with differ-ent percentages of sonicated GO dispersed in dioxane were ultrasounded for 20 min in a VWR USC600TH Ultra-sonic Bath (VWR International). Finally, PCL/dioxane and GO/dioxane solutions were mixed in different proportions (0, 0.1, 0.2 and 0.5 wt% GO) and hand-stirred. The sam-ples were continuously extracted for 30 min at 40 °C to eliminate air and remained under vacuum for seven days to purge all the solvent.

The resulting samples were melted at 80 °C and com-pression molded by a Gumix Model TP-250/200/1-E press. This process was repeated at least twice (rotating the sam-ple) to eliminate any bubbles. Individual cylindrical 4 mm diameter and 0.5 mm average thickness replicates were then drilled. The films were labeled according to GO content (wt%) as follows: PCL (neat PCL), PCL/GO-0.1 (0.1 wt% of GO), PCL/GO-0.2 (0.2 wt% of GO), and PCL/GO-0.5 (0.5 wt% of GO).

2.3. Incubation into Degradation Solutions

Samples of between 6 and 8 mg known dry weight were placed in sealed vials containing 5 mL of a PBS solution in the presence of *PS lipase* and incubated at pH 7.4 and at 37 ± 0.5 °C, on a rotary shaker at 100 rpm. The enzyme concentration was 1 mg/mL of solution medium. Every 8, 24, 48, 72 and 168 hours, three replicates of the solution were washed with distilled water and vacuum-dried at ambient temperature until reaching constant weight.

2.4. Morphology: Field Emission Scanning Electron Microscope (FESEM) and Transmission Electron Microscopy (TEM)

Hybrid morphology was examined on a Zeiss Ultra 55 FESEM, (Zeiss Oxford Instruments, Abingdon, UK) at an acceleration voltage of 2 kV and working distance of 5 mm. The sample surface was sputter-coated with carbon. For the TEM observations, samples were sliced by a cryo-genic Leica EM UC7 (Wetzlar, Germany) ultramicrotome fitted with a Leica EM FC7 low-temperature sectioning system. A Diatome diamond knife was used to section the samples at a temperature around −70 °C, after which they were placed on a copper grid. A JEOL JEM-1010 trans-mission electron microscope took images at 100 kV.

2.5. Weight Loss

After degradation, the samples were dried in a vacuum oven, at room temperature, until constant weight. A Met-tler Toledo semi microbalance with a readability of 0.01 mg was used to weigh the samples. The percentage weight loss was determined by comparing dry weight (w_d) at a specific time with the initial weight (w_0), according to Eq. (1)

$$\text{weight loss } (\%) = \frac{w_0 - w_d}{w_0} \times 100 \qquad (1)$$

2.6. Molecular Weight Analysis by GPC

The weight average molar mass of the samples was deter-mined by gel permeation chromatography at 30 °C on a Waters Breeze GPC system with a 1525 Binary HPLC pump (Waters Corporation, Milford, MA, USA) equipped with a 2414 refractive index detector and Waters Styragel HR THF columns. Tetrahydrofuran (THF) at a flow rate of 1 mL/min was used as the eluent. The calibration curve was prepared according to Shodex monodisperse polystyrene standards (Showa Denko K.K. Kawasaki, Japan). PCL molecular weights were calculated from the Mark-Houwink-Sakurada parameters provided by Huang et al. [59] ($k = 2.9 \cdot 10^{-4}$ [dL/g], $\alpha = 0.7$).

2.7. Differential Scanning Calorimetry (DSC)

The samples thermal properties were studied on an indium-calibrated Mettler Toledo differential scanning calorimeter (DSC, Perkin Elmer, Überlingen, Germany). Samples at room temperature were heated to 100 °C at a scan rate of 10 °C/min and then cooled down to −10 °C at a scan rate of −10 °C/min and reheated again to 100 °C at a scan rate of 10 °C/min. Crystallinity was calculated in the first and second heating scan and cooling scan assum-ing a proportional relationship to the experimental heat of fusion, using a value of 139.5 J/g for the reported heat of fusion 100% crystalline PCL [60].

Production and enzymatic degradation of poly(ε-caprolactone)/GO composites
Martínez-Ramón et al.

Materials Express

2.8. Mechanical Testing

The mechanical properties were measured on a Universal Tensile Testing Machine (Microtest, Deben UK Ltd.) 2000 N load cell at a crosshead speed of 0.4 mm/min. Sheets of about 3.5×1.4 thick, 35 mm length were measured at room temperature. Young's modulus, elongation at break and tensile strength were taken from the stress–strain curves, the Young's modulus being the slope of the linear part of the stress–strain curve in the range between 2 and 8 MPa. Five specimens were tested for each sample and the average values and standard deviation were calculated.

3. RESULTS AND DISCUSSION

3.1. PCL/GO Composites Fabrication

PCL/GO nanocomposites were subjected to enzymatic degradation at 37 °C in a pH 7.4 phosphate buffer solution containing *PS lipase*. The samples were produced following the guidelines of a previous work [56]. The differences with respect to this previous work consisted firstly in the improvement of GO dispersion, for which the sonication process was prolonged and carried out with

a rod sonicator. Secondly, for the final preparation of the samples a steel mold was made and the previously molten material was pressed to eliminate air bubbles and achieve a thinner uniform surface to increase the surface/volume ratio, which affects the percentage of weight loss during degradation, mainly when a surface degradation process is expected.

3.2. Mechanical Testing Prior to Degradation

The mechanical properties under tensile deformation calculated from stress–strain curves are presented in Table I. It can be seen that the elastic modulus increased with GO content, from 1.87 MPa for neat PCL to 3.16 MPa for PCL/GO-0.2 composite. For the PCL/GO-0.5 sample, the Young's modulus increased by about 70% with respect to PCL. These results are in agreement with previous findings which showed that low GO content can raise the elastic modulus [38, 42]. As reported, an increase in the elastic modulus of PCL/GO nanofibers is attributed to the intrinsic properties of the filler, GO dispersion and distribution and adhesion of nanosheets to the PCL matrix [42, 61]. However, adding GO makes the material less elastic and more fragile, as confirmed by the reduced tensile strength and elongation at break (Table I). PCL is able to sustain large deformations. As seen in Table I, adding nanofillers reduced the break elongation, probably due to the lack of interaction between GO nanoparticles and the macromolecular chains. It is worth noting that the changes introduced in the sample preparations with respect to the previous work [56] produced less fragile PCL/GO-0.5 samples, as they could be handled and their mechanical properties could be measured, whereas the same composition in the previous work produced brittle samples.
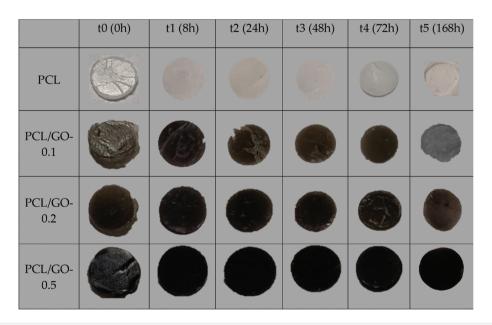
Table I. Elastic modulus, tensile strength, and elongation at break as a function of GO content. The standard deviation is represented in brackets.

Sample	Elastic modulus/ MPa	Tensile strength/ MPa	Elongation at break/%
PCL	1.87 (0.38)	31.70 (0.78)	43.1 (9.7)
PCL/GO-0.1	2.54 (0.36)	12.5 (2.4)	7.55 (0.60)
PCL/GO-0.2	3.16 (0.32)	17.0 (3.9)	10.8 (3.3)
PCL/GO-0.5	3.14 (0.14)	17.2 (6.0)	10.5 (4.9)

Fig. 1. Representative images of samples before degradation and after various degradation times.
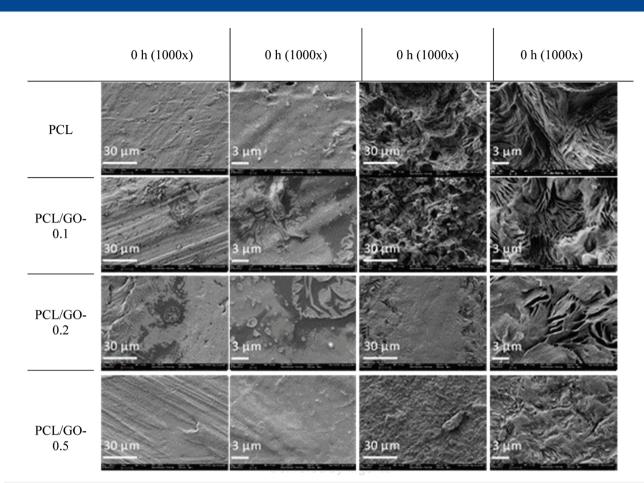
Article

Fig. 2. FESEM images of the neat PCL and PCL/GO composites before starting degradation and after 72 hours of enzymatic degradation at two different magnification levels (white bars represent 30 and 3 microns).

3.3. Morphology: Visual Examination, FESEM and TEM

The macroscopic images of the samples are shown in Figure 1. While the color of the pure PCL sample was white, the composites showed a dark color which became deeper as GO content was increased.

The enzymatic PCL composites were degraded for 168 hours. After immersion, in Figure 1 it can be seen that the degraded samples presented surface irregularities and erosion from the outer edges, which reduced the thickness over degradation time. Surface erosion and formation of voids, cracks, and cavities are signs of the enzyme-induced action, followed by medium penetration into the surface micropores.

The surface morphology of the samples was analyzed by FESEM before and after enzymatic degradation by *PS lipase*. Figure 2 shows FESEM images of the composites before degradation and after 72 hours of degradation in the enzymatic solution. It can be seen that the smoother surface of the non-degraded samples become rougher, with pores and channels, under the enzyme action, showing the crystalline spherulites in relief. After 72 hours of
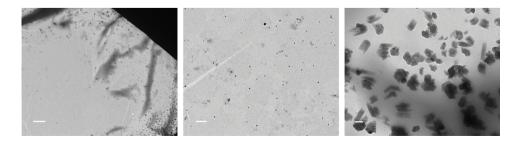

Fig. 3. TEM images of PCL/GO-0.2; (left) at 800×; (center) at 3000×; and (right) at 10000× magnifications. Scale bar represents 5 microns, 500 nm and 100 nm for left, center and right images, respectively.

Production and enzymatic degradation of poly(ε-caprolactone)/GO composites
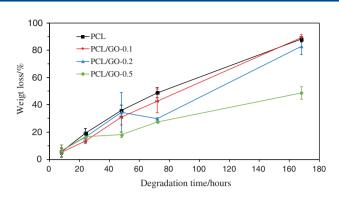Martínez-Ramón et al.

Materials Express

Fig. 4. Weight loss profile as a function of degradation time. Error bars represent standard deviation. Black: Neat PCL; red: PCL/GO-0.1; blue: PCL/GO-0.2; green: PCL/GO-0.5.

degradation, PCL, and PCL/GO-0.1 had rougher surface textures. As degradation progressed, many large distorted pits and caverns appeared. The FESEM PCL/GO-0.2 and PCL/GO-0.5 composite images showed different behavior to that of neat PCL and in the PCL/GO-0.1 composite. In these images (see Fig. 2) these two composites seem to have less surface erosion than the neat PCL and PCL/GO-0.1. After 0.1 wt% higher GO content there seems to be a change in the degradation trend.

Biodegradable polyesters are known to have different degradation kinetics and erosion mechanisms [62–64], the two most predominant pathways being bulk and surface degradation. In surface degradation, diffusion is much slower than the reaction and water enters the polymer at a slower rate than hydrolysis takes place. As a consequence, the sample experiences a thinning effect and this form of degradation is considered advantageous for the controlled supply of drugs, since the surface degradation of a material is more predictable than that of bulk degradation [65]. Visual and FESEM inspection revealed that the overall degradation of the composites was predominantly a surface phenomenon.

TEM images on a nanometric scale provide an observation of the dispersion of nanofillers within the polymeric matrix. A representative TEM image of the PCL/GO-0.2 composite, is shown in Figure 3. It can be seen that the GO is not homogeneously distributed throughout the whole PCL matrix, but is locally well dispersed.

3.4. Weight Loss

The enzymatic degradation of the composites was studied using *PS lipase* in buffer solution. The hydrolysis was followed by mass variations at different degradation times. Figure 4 contains a weight-loss graph as a percentage of the initial mass according to enzymatic degradation time in hours.

Neat PCL was found to degrade fastest (89% weight loss in 168 hours), while the slowest (48% weight loss in 168 hours) was seen in PCL/GO-0.5 composite. The weight loss of the neat PCL, PCL/GO-0.1 and PCL/GO-0.2 composites were quite similar during the first 45 hours of degradation, after which the degradation rate slowed down in the PCL/GO-0.2 composite 83% in 168 hours). Neat PCL showed the fastest enzymatic degradation, while PCL composites degraded more slowly. This behavior could have been caused by the difficulty of the enzymes in reaching the bulk matrix due to the GO barrier properties, which make the diffusion path more tortuous [2, 66]. In addition, a portion of the surface of the specimen in composites is occupied by the filler, so there is less surface available for the enzymes to attack, which in turn slows down surface erosion. These results are in good agreement with similar findings with other aliphatic polymers and other types of fillers [67–68]. In an enzymatic degradation with *PS lipase*, Vidaurre et al. [57] obtained a weight loss of less than 40% in around 168 hours with neat PCL, with a lipase concentration of 0.1 mg/mL of degradation medium. Here, with a lipase concentration of 1 mg/mL of solution, the weight loss was around 80% in 168 hours, corroborating Gan et al. findings [49] that the enzymatic degradation rate of PCL films in PBS with *PS lipase* increased with enzyme concentration.
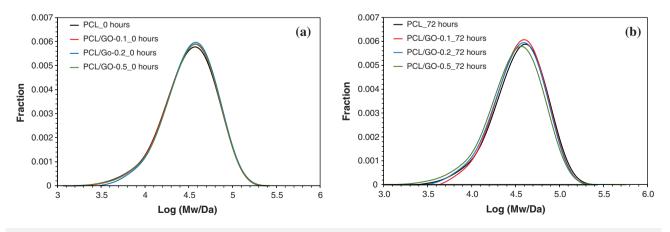

Fig. 5. Molecular weight distribution according to GO content, (a) before degradation and (b) after 72 hours of enzymatic degradation.

Materials Express

Production and enzymatic degradation of poly(ε-caprolactone)/GO composites
Martínez-Ramón et al.

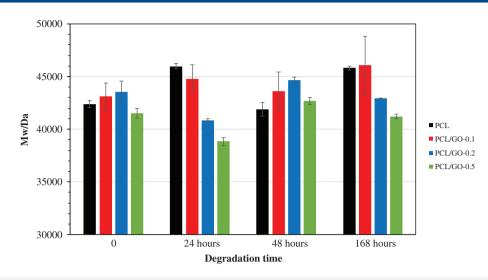**Fig. 6.** Average molecular weight calculated for different degradation times and GO content.

3.5. GPC

Molecular weight changes were monitored by GPC before and during enzymatic degradation. Figure 5 depicts the molecular weight profiles of all the specimens before degradation (a) and after 72 hours of enzymatic degradation (b). As can be seen in Figure 5(a), prior to degradation the weight-average molecular weight, M_w, remained unmodified with the addition of GO filler. A previous study [56] found a progressive decrease in the apparent M_w with increasing added GO content, while similar results were also found when adding GO to different polymers [69–70]. The reason for the reduced M_w with added GO was not totally clear. In the present study, the manufacturing process was refined, adding a second period of sonication with a rod sonicator and also a final compression molding after melting. The result was PCL/GO samples whose molecular weight was not reduced after adding the GO, as was the case in the previous work [56].

After 72 hours of enzymatic degradation, the molecular weights remained unchanged, as can be seen in Figure 5(b). Very slight displacements towards lower M_w can be observed in the PCL/GO-0.2 and PCL/GO-0.5 composites.

Figure 6 shows the weight-average molecular weight obtained by GPC as a function of degradation time for all types of samples. The GPC data showed that molecular weight did not change with degradation time. Although the samples showed a weight loss of around 80% for all samples, except for the PCL/GO-0.5 composite, which had a weight loss of around 40% at 168 hours, as shown in Figure 4, the GPC results showed that no significant changes occurred in the molecular weight after 168 h of enzymatic degradation (Fig. 6). As degradation took place mainly on the surface, any cleaved chains that produced lower molecular weight products would have already been dispersed in the medium.
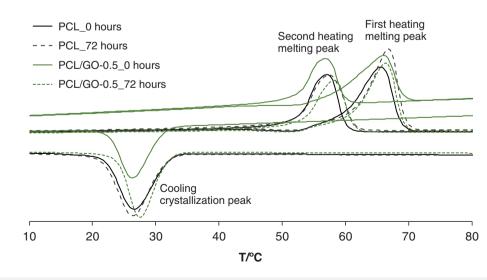

Fig. 7. DSC scans for PCL and PCL/GO-0.5 composite on cooling and first and second heating scan, before and after 72 hours of degradation.

Production and enzymatic degradation of poly(ε-caprolactone)/GO composites
Martínez-Ramón et al.

Materials Express

The molecular weight provided by the GPC test therefore showed no tendency to vary versus degradation time, whereas the presence of hydrophilic GO may facilitate PBS medium infiltration and in turn accelerate PCL degradation. From our molecular weight results, PCL/GO composite degradation seems to offer no obvious evidence of internal autocatalysis. This is consistent with a superficial degradation in which samples are progressively eroded as degradation proceeds while the remaining material maintains its initial properties.

3.6. DSC

Changes in the thermal properties were monitored in relation to GO content and compared using DSC. By way of example, heat flow-temperature curves of a DSC cycle corresponding to neat PCL and a PCL/GO-0.5 composite on cooling and first and second heating scan are shown in Figure 7. The corresponding curves for the same samples after 72 hours in the degradation solution are also shown.

The degree of crystallinity (χ_c), the melting temperature (T_m), calculated during the first and second heating scan, and crystallization peak temperature (T_c), calculated from the cooling scan (T_c) are shown in Table II. It can be seen that, before degradation, crystallinity gradually decreases when adding GO from 67.6% for pure PCL to 50.6% for PCL/GO-0.5 during the first heating scan. Crystallinity also decreases with the addition of GO, during the second heating scan, from 57.4% for pure PCL to 39.8% for PCL/GO-0.5 (Table II). Similar results have been reported in previous studies [38, 39, 43] in which the authors attribute the reduced crystallinity to GO nanoplatelets interacting with PCL molecular chains at the interface, which reduced chain flexibility and retarded crystallization. However, other studies have found that crystallinity rose steadily when GO was added [71–73]. Other studies concluded that graphene increases the number of crystallization nucleation sites, which affects the size and number of spherulite crystalline regions in polycaprolactone [74]. This double effect of fillers on polymeric matrix crystallinity can be explained as follows: on one hand, they act as nucleating agents, favoring the formation of crystallization nuclei and therefore increasing the crystallization rate, while on the other, the presence of inorganic

particles can interfere with the movement of macromolecular chains, interfering with their regular alignment [75]. The reduced crystallinity (χ_c) could thus be assigned to the interfacial interaction between PCL molecular chains and GO nanoplatelets, which reduces chain flexibility and slows down crystallization, even though GO provides heterogeneous nuclei for PCL crystallization [38].

The effect of GO content on PCL matrix crystallization when cooling can be observed from DSC traces (Fig. 7). Before degradation T_c increased by about 2 °C in the case of PCL/GO-0.1, while it remained unchanged in the rest of the composites (Table II). The increase in T_c could mean that GO filler is an efficient nucleating agent for PCL crystallization, as found by Hua et al. in a study of GO reinforced poly(L-lactide) nanocomposites [76].

After 72 hours of enzymatic degradation, the crystallization temperatures (T_c) of all the composites increased slightly (less than 4 °C) compared to that of neat PCL, as can be seen in Table III. The higher T_c on adding GO shows that the dispersed GO nanosheets probably acted as efficient nucleating seeds and helped to promote PCL crystallization during degradation due to the formation of smaller molecular chains entrapped in the polymer matrix. DSC data also show that adding GO to the PCL structure did not significantly affect the melting temperature (T_m) of the composites with respect to neat PCL (Table II), in agreement with some earlier studies [71, 77]. Since the PCL/GO composites' melting temperature hardly changed, it was not significantly affected by adding GO. Degradation over 72 hours results in no change in the T_m for neat PCL or composites, which change less than 2 °C (Fig. 7 and Table III).

GO reinforces polymers thanks to the intrinsic properties of its nanolayers, its dispersion in the polymer matrix, interfacial interactions and different crystalline structures [61]. PCL/GO composites showed better mechanical behavior than neat PCL in terms of a higher Young's modulus, which only increased with the presence of GO nanosheets (Table I), as has also been found by other authors [78]. Prior to degradation, most of its thermal properties were only slightly influenced, except for crystallinity, as can be seen in Table II.

Table II. Degree of crystallinity (χ), melting peak temperature (T_m) of the first and second heating scan, crystallinity (χ_c) and crystallization temperature (T_c) on cooling, before degradation.

	0 hours					
	First heating		Cooling		Second heating	
Sample	χ (%)	T_{m1} (°C)	χ_c (%)	T_c (°C)	χ (%)	T_{m2} (°C)
PCL	67.60	65.46	51.90	26.65	57.40	56.96
PCL/GO-0.1	64.20	65.56	47.70	28.62	54.50	57.21
PCL/GO-0.2	62.30	64.73	48.90	26.29	53.40	56.99
PCL/GO-0.5	50.60	66.03	39.40	26.29	39.80	56.90

Table III. Degree of crystallinity (χ), melting peak temperature (T_m) of the first and second heating scan, crystallinity (χ_c) and crystallization temperature (T_c) on cooling after 72 hours of enzymatic degradation.

	72 hours					
	First heating		Cooling		Second heating	
Sample	χ (%)	T_{m1} (°C)	χ_c (%)	T_c (°C)	χ (%)	T_{m2} (°C)
PCL	75.50	66.79	42.00	26.30	64.90	57.33
PCL/GO-0.1	61.10	66.50	44.80	29.60	46.50	58.46
PCL/GO-0.2	63.90	67.48	47.10	26.62	51.70	58.43
PCL/GO-0.5	62.10	66.28	45.70	27.60	54.20	58.38

Materials Express

Production and enzymatic degradation of poly(ε-caprolactone)/GO composites
Martínez-Ramón et al.

PCL film has been reported to degrade completely in a few days in phosphate buffer solution containing *PS lipase*. During enzymatic degradation, PCL film crystallinity was gradually reduced and degradation took place in both the amorphous phase and crystalline region [49]. In the present study, the reduced crystallinity in PCL/GO composites before degradation was proportional to the GO percentage, both in the first and second scans. The higher the GO content the larger the drop in crystallinity (see Table II). However, during enzymatic degradation the decrease in crystallinity was not proportional to the GO percentage. The PCL/GO-0.1 composite lost most crystallinity during degradation. At higher GO contents the trend was reversed and crystallinity increased, always remaining lower than that of pure PCL, as can be seen in Table III. Some authors have found the critical value of the GO percentage in PCL/GO nanofiber to be 0.1 wt% [42], which agrees with our findings.

As polyester enzymatic degradation is known to occur through ester bond hydrolysis, the degradation rate is associated with water's wetting ability and its subsequent penetration into the nanocomposites. As a consequence, one might think that the hydrophilic or hydrophobic character of the "filler" could have a great influence on the extent to which hydrolysis occurs. Bikiaris et al. [44] studied the correlation of non-GO nanofiller hydrophilicity with enzymatic hydrolysis rate and concluded that it does not play an important role in the degree of enzymatic hydrolysis. As can be concluded from the above results, despite GO's highly hydrophilic character [14, 19], all our composites had a slower degradation rate than neat PCL, also indicating that the GO filler hydrophilicity does not favor the enzymatic degradation rate. Furthermore, from the morphology, GPC and calorimetric results, the most predominant degradation pathway seems to be surface degradation.

4. CONCLUSIONS

A series of PCL composites were prepared with different GO filler contents (0.1, 0.2 and 0.5% w/w GO/PCL) to characterize their properties and evaluate their enzymatic degradation by the action of *Pseudomonas lipase*. The composites were produced by the solution mixing method, followed by compression molding into films. Stress–strain testing showed that tensile strength and elongation at break decreased with higher amounts of GO filler, while the elastic modulus increased as GO content was raised. It can therefore be concluded that adding GO makes PCL composites less ductile but stronger. Prior to degradation, crystallinity gradually decreases when adding GO from 67.6% for pure PCL to 50.6% for PCL/GO-0.5 during the first heating scan. The decrease in crystallinity could be assigned to the interfacial interaction between PCL molecular chains and GO nanoplatelets, which reduces the

chain's flexibility and slows down the crystallization process, even though GO provides heterogeneous nuclei for PCL crystallization. The composites' melting temperature was unaffected by either GO addition or degradation.

Enzymatic degradation can be used to study the morphological and chemical changes that take place during degradation in a reasonable period of time, as PCL is known to fully degrade in little more than two years. The degradation results indicated that the enzymatic degradation was inversely proportional to GO content. At least 75% of the weight was lost after 168 hours, except in the PCL/GO-0.5 composite (48%) over a 168-hour period. The GPC data showed that the molecular weight did not change with degradation time. The molecular weight, morphology and calorimetry results suggest that degradation took place only on the surface.

References and Notes

1. Gandini, A., **2008**. Polymers from renewable resources: A challenge for the future of macromolecular materials. *Macromolecules, 41*, pp.9491–9504.
2. Bikiaris, D.N., **2013**. Nanocomposites of aliphatic polyesters: An overview of the effect of different nano fillers on enzymatic hydrolysis and biodegradation of polyesters. *Polymer Degradation and Stability, 98*, pp.1908–1928.
3. Kweon, H., Yoo, M.K., Park, I.K., Kim, T.H., Lee, H.C., Lee, H.-S., Oh, J.-S., Akaike, T. and Cho, C.S., **2003**. A novel degradable polycaprolactone networks for tissue engineering. *Biomaterials, 24*, pp.801–808.
4. Woodruff, M.A. and Hutmacher, D.W., **2010**. The return of a forgotten polymer—Polycaprolactone in the 21st century. *Progress in Polymer Science, 35*, pp.1217–1256.
5. Joseph, J.-G., **2006**. Polymers for tissue engineering, medical devices, and regenerative medicine. Concise general review of recent studies. *Polymers for Advanced Technologies, 17*, pp.395–418.
6. Ju, J., Peng, X., Huang, K., Li, L., Liu, X., Chitrakar, C., Chang, L., Gu, Z. and Kuang, T., **2019**. High-performance porous PLLA-based scaffolds for bone tissue engineering: Preparation, characterization, and in vitro and in vivo evaluation. *Polymer, 180*, p.121707.
7. Gao, S., Tang, G., Hua, D., Xiong, R., Han, J., Jiang, S., Zhang, Q. and Huang, C., **2019**. Stimuli-responsive bio-based polymeric systems and their applications. *Journal of Materials Chemistry B, 7*, pp.709–729.

Production and enzymatic degradation of poly(ε-caprolactone)/GO composites
Martínez-Ramón et al.

Materials Express

8. Chen, Q., Yang, Y., Lin, X., Ma, W., Chen, G., Li, W., Wang, X. and Yu, Z., **2018**. Platinum (IV) prodrugs with long lipid chains for drug delivery and overcoming cisplatin resistance. *Chemical Communications, 54*(42), pp.5369–5372.

9. Yu, Y., Xu, Q., He, S., Xiong, H., Zhang, Q., Xu, W., Ricotta, V., Bai, L., Zhang, Q., Yu, Z., Ding, J., Xiao, H. and Zhou, D., **2019**. Recent advances in delivery of photosensitive metal-based drugs. *Coordination Chemistry Reviews, 387*, pp.154–179.

10. Huang, K., Wu, J. and Gu, Z., **2019**. Black phosphorus hydrogel scaffolds enhance bone regeneration via a sustained supply of calcium-free phosphorus. *ACS Applied Materials & Interfaces, 11*(3), pp.2908–2916.

11. Armentano, I., Dottori, M., Fortunati, E., Mattioli, S. and Kenny, J.M., **2010**. Biodegradable polymer matrix nanocomposites for tissue engineering: A review. *Polymer Degradation and Stability, 95*, pp.2126–2146.

12. Murariu, M., Ferreira, A.D.S., Vittoria, V., Dubois, P., Gorrasi, G. and Alexandre, M., **2008**. Effect of filler content and size on transport properties of water vapor in PLA/calcium sulfate composites. *Biomacromolecules, 9*(3), pp.984–990.

13. Torre, L., Stadler, H., Mondragon, I., Tercjak, A., Kenny, J.M., Peponi, L. and Gutierrez, J., **2008**. Self-assembling of SBS block copolymers as templates for conductive silver nanocomposites. *Macromolecular Materials and Engineering, 293*(7), pp.568–573.

14. Dreyer, D.R., Park, S., Bielawski, C.W. and Ruoff, R.S., **2010**. Graphite oxide. *Chemical Society Reviews, 39*(1), pp.228–240.

15. Brodie, B.C., **1860**. Sur le poids atomique du graphite. *Annales de Chimie et de Physique, 59*, pp.466–472.

16. Dimiev, A., Kosynkin, D.V., Alemany, L.B., Chaguine, P. and Tour, J.M., **2012**. Pristine graphite oxide. *Journal of the American Chemical Society, 134*(5), pp.2815–2822.

17. Dimiev, A.M., Alemany, L.B. and Tour, J.M., **2013**. Graphene oxide. Origin of acidity, its instability in water, and a new dynamic structural model. *ACS Nano, 7*(1), pp.576–588.

18. Potts, J.R., Dreyer, D.R., Bielawski, C.W. and Ruoff, R.S., **2011**. Graphene-based polymer nanocomposites. *Polymer, 52*(1), pp.5–25.

19. Buchsteiner, A., Lerf, A. and Pieper, J., **2006**. Water dynamics in graphite oxide investigated with neutron scattering. *Journal of Physical Chemistry B, 110*(45), pp.22328–22338.

20. Konios, D., Stylianakis, M.M., Stratakis, E. and Kymakis, E., **2014**. Dispersion behaviour of graphene oxide and reduced graphene oxide. *Journal of Colloid and Interface Science, 430*, pp.108–112.

21. Kuilla, T., Bhadra, S., Yao, D., Kim, N.H., Bose, S. and Lee, J.H., **2010**. Recent advances in graphene based polymer composites. *Progress in Polymer Science, 35*(11), pp.1350–1375.

22. Yang, X., Tu, Y., Li, L., Shang, S. and Tao, X.M., **2010**. Well-dispersed chitosan/graphene oxide nanocomposites. *ACS Applied Materials & Interfaces, 2*(6), pp.1707–1713.

23. Bao, C., Guo, Y., Song, L. and Hu, Y., **2011**. Poly(vinyl alcohol) nanocomposites based on graphene and graphite oxide: A comparative investigation of property and mechanism. *Journal of Materials Chemistry, 21*, pp.13942–13950.

24. Han, D., Yan, L., Chen, W. and Li, W., **2011**. Preparation of chitosan/graphene oxide composite film with enhanced mechanical strength in the wet state. *Carbohydrate Polymers, 83*(2), pp.653–658.

25. Kulkarni, D.D., Choi, I., Singamaneni, S.S. and Tsukruk, V.V., **2010**. Graphene oxide—Polyelectrolyte nanomembranes. *ACS Nano, 4*, pp.4667–4676.

26. Liang, J., Huang, Y., Zhang, L., Wang, Y., Ma, Y., Cuo, T. and Chen, Y., **2009**. Molecular-level dispersion of graphene into poly(vinyl alcohol) and effective reinforcement of their nanocomposites. *Advanced Functional Materials, 19*(14), pp.2297–2302.

27. Luong, N.D., Hippi, U., Korhonen, J.T., Soininen, A.J., Ruokolainen, J., Johansson, L.S., Nam, J.D., Sinh, L.H. and Seppälä, J., **2011**. Enhanced mechanical and electrical properties of polyimide film by graphene sheets via in situ polymerization. *Polymer, 52*(23), pp.5237–5242.

28. Salavagione, H.J., Gómez, M.A. and Martínez, G., **2009**. Polymeric modification of graphene through esterification of graphite oxide and poly(vinyl alcohol). *Macromolecules, 42*(17), pp.6331–6334.

29. Xu, Z. and Gao, C., **2010**. In situ polymerization approach to graphene-reinforced nylon-6 composites. *Macromolecules, 43*(16), pp.6716–6723.

30. Tang, L.C., Wan, Y.J., Yan, D., Pei, Y.B., Zhao, L., Li, Y.B., Wu, L.B., Jian, J.X. and Lai, G.Q., **2013**. The effect of graphene dispersion on the mechanical properties of graphene/epoxy composites. *Carbon, 60*, pp.16–27.

31. Wang, X. Wan, F., Zhang, L., Zhao, Z., Niu, Z. and Chen, J., **2018**. Large-area reduced graphene oxide composite films for flexible asymmetric sandwich and microsized supercapacitors. *Advanced Functional Materials, 28*, p.1707247.

32. Li, Y., Jing, T., Xu, G., Tian, J., Dong, M., Shao, Q., Wang, B., Wang, Z., Zheng, Y., Yang, C. and Guo, Z., **2018**. 3-D magnetic graphene oxide-magnetite poly(vinyl alcohol) nanocomposite substrates for immobilizing enzyme. *Polymer, 149*, pp.13–22.

33. Diban, N., Sánchez-González, S., Lázaro-Díez, M., Ramos-Vivas, J. and Urtiaga, A., **2017**. Facile fabrication of Poly(ε-caprolactone)/graphene oxide membranes for bioreactors in tissue engineering. *Journal of Membrane Science, 540*, pp.219–228.

34. Kim, H., Miura, Y. and MacOsko, C.W., **2010**. Graphene/polyurethane nanocomposites for improved gas barrier and electrical conductivity. *Chemistry of Materials, 22*(11), pp.3441–3450.

35. Song, Y.S. and Youn, J.R., **2005**. Influence of dispersion states of carbon nanotubes on physical properties of epoxy nanocomposites. *Carbon, 43*, pp.1378–1385.

36. Ahmad, H., Fan, M. and Hui, D., **2018**. Graphene oxide incorporated functional materials: A review. *Composites Part B: Engeneering, 145*, pp.270–280.

37. Li, Y., Liao, C. and Tjong, S.C., **2019**. Synthetic biodegradable aliphatic polyester nanocomposites reinforced with nanohydroxyapatite and/or graphene oxide for bone tissue engineering applications. *Nanomaterials, 9*(4), p.590.

38. Wan, C. and Chen, B., **2011**. Poly(ε-caprolactone)/graphene oxide biocomposites: Mechanical properties and bioactivity. *Biomedical Materials, 6*(5), pp.055010–055017.

39. Kai, W., Hirota, Y., Hua, L. and Inoue, Y., **2008**. Thermal and mechanical properties of a poly(ε-caprolactone)/graphite oxide composite. *Journal of Applied Polymer Science, 107*, pp.1395–1400.

40. Kumar, S., Raj, S., Kolanthai, E., Sood, A.K.K., Sampath, S. and Chatterjee, K., **2015**. Chemical functionalization of graphene to augment stem cell osteogenesis and inhibit biofilm formation on polymer composites for orthopedic applications. *ACS Applied Materials & Interfaces, 7*(5), pp.3237–3252.

41. Song, J., Gao, H., Zhu, G., Cao, X., Shi, X. and Wang, Y., **2015**. The preparation and characterization of polycaprolactone/graphene oxide biocomposite nanofiber scaffolds and their application for directing cell behaviors. *Carbon, 95*, pp.1039–1050.

42. Ramazani, S. and Karimi, M., **2015**. Aligned poly(ε-caprolactone)/graphene oxide and reduced graphene oxide nanocomposite nanofibers: Morphological, mechanical and structural properties. *Materials Science and Engineering C, 56*, pp.325–334.

43. Balkova, R., Hermanova, S., Voberkova, S., Damborsky, P., Richtera, L., Omelkova, J. and Jancar, J., **2014**. Structure and morphology of microbial degraded poly(e-caprolactone)/graphite oxide composite. *Journal of Polymers and the Environment, 22*, pp.190–199.

44. Bikiaris, D.N., Nianias, N.P., Karagiannidou, E.G. and Docoslis, A., **2012**. Effect of different nanoparticles on the properties and enzymatic hydrolysis mechanism of aliphatic polyesters. *Polymer Degradation and Stability, 97*, pp.2077–2089.

Article

Materials Express

Production and enzymatic degradation of poly(ε-caprolactone)/GO composites
Martínez-Ramón et al.

Article

45. Sánchez-González, S., Diban, N. and Urtiaga, A., **2018**. Hydrolytic degradation and mechanical stability of poly(ε-caprolactone)/reduced graphene oxide membranes as scaffolds for in vitro neural tissue regeneration. *Membranes, 8*(1), p.12.

46. Vert, M., Li, S.M., Spenlehauer, G. and Guerin, P., **1992**. Bioresorbability and biocompatibility of aliphatic polyesters. *Journal of Materials Science: Materials in Medicine, 3*(6), pp.432–446.

47. Papageorgiou, G.Z. and Bikiaris, D.N., **2007**. Synthesis, cocrystallization, and enzymatic degradation of novel poly(butylene-co-propylene succinate) copolymers. *Biomacromolecules, 8*(8), pp.2437–2449.

48. Gan, Z., Donghong, Y., Zhong, Z., Liang, Q. and Jing, X., **1999**. Enzymatic degradation of poly(ε-caprolactone)/poly(dl-lactide) blends in phosphate buffer solution. *Polymer, 40*(10), pp.2859–2862.

49. Gan, Z., Liang, Q., Zhang, J. and Jing, X., **1997**. Enzymatic degradation of poly(ε-caprolactone) film in phosphate buffer solution cotaining lipases. *Polymer Degradation and Stability, 56*(2), pp.209–213.

50. Mochizuki, M., Hirano, M., Kanmuri, Y., Kudo, K. and Tokiwa, Y., **1995**. Hydrolysis of polycaprolactone fibers by lipase: Effects of draw ratio on enzymatic degradation. *Journal of Applied Polymer Science, 55*(2), pp.289–296.

51. Lee, C.W., Kimura, Y. and Chung J.D., **2008**. Mechanism of enzymatic degradation of poly(butylene succinate). *Macromolecular Research, 16*(7), pp.651–658.

52. Castilla-Cortázar, I., Más-Estellés, J., Meseguer-Dueñas, J.M., Escobar Ivirico, J.L., Marí, B. and Vidaurre, A., **2012**. Hydrolytic and enzymatic degradation of a poly(ε-caprolactone) network. *Polymer Degradation and Stability, 97*(8), pp.1241–1248.

53. He, F., Li, S., Vert, M. and Zhuo, R., **2003**. Enzyme-catalyzed polymerization and degradation of copolymers prepared from ε-caprolactone and poly(ethylene glycol). *Polymer, 44*(18), pp.5145–5151.

54. Fukuzaki, M.K.H., Yoshida, M. and Asano, M.K., **1990**. Synthesis of low-molecular-weight copoly(L-lactic acid/e-caprolactone) by direct copolycondensation in the absence of catalysts, and enzymatic degradation of the polymers. *Polymer, 31*, pp.2006–2014.

55. Sun, H., Mei, L., Song, C., Cui, X. and Wang, P., **2006**. The in vivo degradation, absorption and excretion of PCL-based implant. *Biomaterials, 27*, pp.1735–1740.

56. Castilla-Cortázar, I., Vidaurre, A., Mari, B. and Campillo-Fernández, A.J., **2019**. Morphology, crystallinity, and molecular weight of poly(ε-caprolactone)/graphene oxide hybrids. *Polymers, 11*(7), p.1099.

57. Vidaurre, A., Duenas, J.M.M., Estelles, J.M. and Cortazar, I.C., **2008**. Influence of enzymatic degradation on physical properties of poly(epsilon-caprolactone) films and sponges. *Macromolecular Symposia, 269*, pp.38–46.

58. Sailema-Palate, G.P., Vidaurre, A., Campillo-Fernández, A.J. and Castilla-Cortázar, I., **2016**. A comparative study on poly(ε-caprolactone) film degradation at extreme pH values. *Polymer Degradation and Stability, 130*, pp.118–125.

59. Huang, Y., Xu, Z., Huang, Y., Ma, D., Yang, J. and Mays, J.W., **2003**. Characterization of poly(ε-caprolactone) via size exclusion chromatography with online right-angle laser-light scattering and viscometric detectors. *International Journal of Polymer Analysis and Characterization, 8*(6), pp.383–394.

60. Crescenzi, V., Manzini, G., Calzolari, G. and Borri, C., **1972**. Thermodynamics of fusion of poly-beta-propiolactone and poly-ε-caprolactone. Comparative analysis of the melting of aliphatic polylactone and polyester chains. *European Polymer Journal, 8*(3), pp.449–463.

61. Wan, C. and Chen, B., **2012**. Reinforcement and interphase of polymer/graphene oxide nanocomposites. *Journal of Materials Chemistry, 22*(8), pp.3637–3646.

62. Grizzi, I., Garreau, H., Li, S. and Vert, M., **1995**. Hydrolytic degradation of devices based on poly(DL-lactic acid) size dependence. *Biomaterials, 16*(4), pp.305–311.

63. Burkersroda, F. Von, Schedl, L. and Göpferich, A., **2002**. Why degradable polymers undergo surface erosion or bulk erosion. *Biomaterials, 23*(21), pp.4221–4231.

64. Lam, C.X., Savalani, M.M., Teoh, S.H. and Hutmacher, D.W., **2008**. Dynamics of in vitro polymer degradation of polycaprolactone-based scaffolds: Accelerated versus simulated physiological conditions. *Biomedical Materials, 3*(3), p.034108.

65. Göpferich, A. and Langer, R., **1993**. Modeling of polymer erosion. *Macromolecules, 26*(16), pp.4105–4112.

66. Nerantzaki, M., Papageorgiou, G.Z. and Bikiaris, D.N., **2014**. Effect of nanofiller's type on the thermal properties and enzymatic degradation of poly(ε-caprolactone). *Polymer Degradation and Stability, 108*, pp.257–268.

67. Lee, S.R., Park, H.M., Lim, H., Kang, T., Li, X., Cho, W.J. and Ha, C.S., **2002**. Microstructure, tensile properties, and biodegradability of aliphatic polyester clay nanocomposites. *Polymer, 43*, pp.2495–2500.

68. Fukushima, K., Tabuani, D., Abbate, C., Arena, M. and Rizzarelli, P., **2011**. Preparation, characterization and biodegradation of biopolymer nanocomposites based on fumed silica. *European Polymer Journal, 47*, pp.139–152.

69. Arza, C.R., Jannasch, P. and Maurer, F.H., **2014**. Network formation of graphene oxide in poly(3-hydroxybutyrate) nanocomposites. *European Polymer Journal, 59*, pp.262–269.

70. Larsson, M., Hetherington, C.J.D., Wallenberg, R. and Jannasch, P., **2017**. Effect of hydrophobically modified graphene oxide on the properties of poly(3-hydroxybutyrate-co-4-hydroxybutyrate). *Polymer, 108*, pp.66–77.

71. Wang, G.S., Zhi-Yong, W., Lin, S., Chen, G., Zhang, W., Dong, X. and Qi, M., **2013**. Morphology, crystallization and mechanical properties of poly(ε-caprolactone)/graphene oxide nanocomposites. *Chinese Journal of Polymer Science (English Edition), 31*(8), pp.1148–1160.

72. Kumar, S., Azam, D., Raj, S., Kolanthai, E., Vasu, K.S., Sood, A.K. and Chatterjee, K., **2016**. 3D scaffold alters cellular response to graphene in a polymer composite for orthopedic applications. *Journal of Biomedical Materials Research—Part B Applied Biomaterials, 104*(4), pp.732–749.

73. Hua, L., Kai, W.H. and Inoue, Y., **2007**. Crystallization behavior of poly(ε-caprolactone)/graphite oxide composites. *Journal of Applied Polymer Science, 106*, pp.4225–4232.

74. Sayyar, S., Murray, E., Thompson, B.C., Gambhir, S., Officer, D.L. and Wallace, G.G., **2013**. Covalently linked biocompatible graphene/polycaprolactone composites for tissue engineering. *Carbon, 52*, pp.296–304.

75. Marega, C. and Marigo, A., **2015**. Effect of electrospun fibers of polyhydroxybutyrate filled with different organoclys on morphology, biodegradation, and thermal stability of poly(e-caprolactona). *Journal of Applied Polymer Science, 42342*, pp.1–12.

76. Hua, L., Kai, W., Yang, J. and Inoue, Y., **2010**. A new poly(l-lactide)-grafted graphite oxide composite: Facile synthesis, electrical properties and crystallization behaviors. *Polymer Degradation and Stability, 95*(12), pp.2619–2627.

77. Yıldırım, S., Demirtaş, T.T., Dinçer, C.A., Yıldız, N. and Karakeçili, A., **2018**. Preparation of polycaprolactone/graphene oxide scaffolds: A green route combining supercritial CO₂ technology and porogen leaching. *The Journal of Supercritical Fluids, 133*, pp.156–162.

78. Wang, H., Domingos, M. and Scenini, F., **2018**. Advanced mechanical and thermal characterization of 3D bioextruded poly(ε-caprolactone)-based composites. *Rapid Prototyping Journal, 24*(4), pp.731–738.